CellPress

Cell Host & Microbe
Article

Convergent Targeting of a Common Host Protein-Network by Pathogen Effectors from Three Kingdoms of Life

Ralf Weßling,[1,18] Petra Epple,[2,14,18] Stefan Altmann,[3,18] Yijian He,[2,15,18] Li Yang,[2,18] Stefan R. Henz,[4] Nathan McDonald,[2] Kristin Wiley,[2] Kai Christian Bader,[5] Christine Gläßer,[5,16] M. Shahid Mukhtar,[2,6] Sabine Haigis,[1] Lila Ghamsari,[7,17] Amber E. Stephens,[1] Joseph R. Ecker,[8] Marc Vidal,[7] Jonathan D.G. Jones,[9] Klaus F.X. Mayer,[5] Emiel Ver Loren van Themaat,[1] Detlef Weigel,[4] Paul Schulze-Lefert,[1] Jeffery L. Dangl,[2,10,11,12,*] Ralph Panstruga,[1,13,*] and Pascal Braun[3,*]

[1]Department of Plant Microbe Interactions, Max Planck Institute for Plant Breeding Research, Cologne, D-50829, Germany
[2]Howard Hughes Medical Institute and Department of Biology, University of North Carolina at Chapel Hill, Chapel Hill, NC 27599, USA
[3]Technische Universität München (TUM), Center for Life and Food Sciences Weihenstephan, Department for Plant Systems Biology, D-85354 Freising, Germany
[4]Department of Molecular Biology, Max Planck Institute for Developmental Biology, D-72076 Tübingen, Germany
[5]Plant Genome and Systems Biology, Helmholtz Zentrum München, D-85764 Neuherberg, Germany
[6]Department of Biology, University of Alabama Birmingham, Birmingham, AL 35294, USA
[7]Center for Cancer Systems Biology (CCSB) and Department of Cancer Biology, Dana Farber Cancer Institute, and Harvard Medical School, Department of Genetics, Boston, MA 02215, USA
[8]Howard Hughes Medical Institute and Salk Institute for Biological Studies, Plant Biology Lab, La Jolla, CA 92037, USA
[9]The Sainsbury Laboratory, John Innes Centre, Norwich Research Park, Colney Lane, Norwich NR4 7UH, UK
[10]Curriculum in Genetics and Molecular Biology, University of North Carolina at Chapel Hill, Chapel Hill, NC 27599, USA
[11]Carolina Center for Genome Science, University of North Carolina at Chapel Hill, Chapel Hill, NC 27599, USA
[12]Department of Microbiology and Immunology, University of North Carolina at Chapel Hill, Chapel Hill, NC 27599, USA
[13]Rheinisch Westfälische Technische Hochschule (RWTH) Aachen University, Institute for Biology I, Unit of Plant Molecular Cell Biology, D-52074 Aachen, Germany
[14]Present address: BASF Plant Science LP, Research Triangle Park, NC 27709, USA
[15]Present address: Department of Plant Pathology, NC State University, Raleigh, NC 27695, USA
[16]Present address: Zentrum für Molekulare Biologie der Universität Heidelberg, D-69120 Heidelberg, Germany
[17]Present address: Department of Systems Biology, Columbia University, New York, NY 10032, USA
[18]Co-first Authors
*Correspondence: dangl@email.unc.edu (J.L.D.), panstruga@bio1.rwth-aachen.de (R.P.), pbraun@wzw.tum.de (P.B.)
http://dx.doi.org/10.1016/j.chom.2014.08.004

SUMMARY

While conceptual principles governing plant immunity are becoming clear, its systems-level organization and the evolutionary dynamic of the host-pathogen interface are still obscure. We generated a systematic protein-protein interaction network of virulence effectors from the ascomycete pathogen *Golovinomyces orontii* and *Arabidopsis thaliana* host proteins. We combined this data set with corresponding data for the eubacterial pathogen *Pseudomonas syringae* and the oomycete pathogen *Hyaloperonospora arabidopsidis*. The resulting network identifies host proteins onto which intraspecies and interspecies pathogen effectors converge. Phenotyping of 124 *Arabidopsis* effector-interactor mutants revealed a correlation between intraspecies and interspecies convergence and several altered immune response phenotypes. Several effectors and the most heavily targeted host protein colocalized in subnuclear foci. Products of adaptively selected *Arabidopsis* genes are enriched for interactions with effector targets. Our data suggest the existence of a molecular host-pathogen interface that is conserved across *Arabidopsis* accessions, while evolutionary adaptation occurs in the immediate network neighborhood of effector targets.

INTRODUCTION

The spread of pathogens is predicted to change in the wake of global warming, generating emerging epidemics threatening human welfare and security. Plants evolved a sophisticated two-layered defense system to detect and defend against the majority of potential pathogens (Chisholm et al., 2006; Dodds and Rathjen, 2010; Jones and Dangl, 2006). Activation of plant pattern-recognition receptor kinases by highly conserved microbe-associated molecular patterns (MAMPs) triggers a complex cellular response termed MAMP-triggered immunity (MTI) that can stop microbial proliferation. Host-adapted pathogens are equipped with diverse suites of virulence effectors, which are delivered into the plant cell by various and mostly poorly understood means. Effector proteins interact with host proteins to undermine MTI and to modify host physiology, thus

enhancing pathogen proliferation (Feng and Zhou, 2012; Raffaele and Kamoun, 2012; Win et al., 2012). Plants evolved highly polymorphic intracellular nucleotide-binding site, leucine-rich repeat (NLR) proteins to recognize intracellular effectors. Activation of NLRs is also poorly understood in all but a few cases, but it can proceed by either direct effector-NLR interaction or upon effector modification of an NLR-associated host target protein. NLR activation results essentially in a more rapid and higher amplitude MTI output known as effector-triggered immunity (Chisholm et al., 2006; Dodds and Rathjen, 2010; Jones and Dangl, 2006).

While the conceptual principles of the plant immune system have been elucidated, knowledge of its systems-level organization and the evolutionary dynamic of the molecular host-pathogen interface are rudimentary. Filling this gap represents an important goal in the quest for targeted crop improvement (Dangl et al., 2013; Pardey et al., 2013). The reference eudicot *Arabidopsis thaliana* (hereafter *Arabidopsis*) is host to a range of evolutionarily diverse pathogens, including bacteria, oomycetes, and fungi. We defined an effector-host network featuring protein interactions between effectors from the oomycete *Hyaloperonospora arabidopsidis* (*Hpa*) and the eubacterium *Pseudomonas syringae* (*Psy*) and 8,000 *Arabidopsis* host proteins and integrated this with a first-generation *Arabidopsis* interactome map (Consortium, 2011; Mukhtar et al., 2011). Our results suggested that effectors from these evolutionarily diverse pathogens converge onto common host proteins, which were characterized by a high interaction degree and a central position in the host protein network. Immune function was demonstrated for 15 of 17 tested proteins that are effector targets shared by both pathogens (Mukhtar et al., 2011). It remained to be determined whether the effector convergence onto common targets extended to *Arabidopsis* pathogens from other kingdoms from the microbial tree of life, how effector convergence related broadly to phenotypic relevance, and how the central network position of many targeted host proteins accommodated the selective pressure imposed by pathogens.

While the effector set of facultative phytopathogenic bacteria like *Psy* is confined to 10–40 effectors per strain (Baltrus et al., 2011), the genomes of eukaryote obligate biotrophic plant pathogens encode extensive apparent effector arsenals (Baxter et al., 2010; Raffaele and Kamoun, 2012; Win et al., 2012). Only a minute fraction of these are functionally characterized, largely because genetic screens are challenging or as yet impossible in most of these organisms. The increased availability of genome sequences and improved bioinformatic prediction pipelines facilitate identification of proteins carrying signatures of virulence effectors. Recent additions include the powdery mildew fungi, an economically important class of plant pathogens with annotated candidate effector repertoires in several species, strains, and *formae speciales* (Hacquard et al., 2013; Pedersen et al., 2012; Wicker et al., 2013). The obligate biotrophic ascomycete *Golovinomyces orontii* (*Gor*) causes powdery mildew on *Arabidopsis* (Micali et al., 2008). The available genome resources make *Gor* an excellent pathogen to identify effectors and their interacting host proteins. Additionally, this ascomycete belongs to a different taxonomic kingdom than the eubacterium *Psy* and the stramenopile *Hpa* (Figure 1A), providing an evolutionary contrast from which to challenge the principles we previously proposed regarding the structure of a plant-pathogen interactome network (Mukhtar et al., 2011).

RESULTS

Definition and Cloning of Candidate *Golovinomyces orontii* Virulence Effectors

We identified *Gor* effector candidates (*OECs*) iteratively using a bioinformatic pipeline (Figure 1B). Using several criteria, including a size cutoff; presence of an N-terminal secretion signal; and, due to the rapidly evolving nature of effectors, a lack of homology outside the powdery mildew fungi; we predicted 103 *OECs* de novo from a sequenced haustorial *Gor* cDNA library (Weßling et al., 2012). This set of *OECs*, and candidate effector sequences from the barley powdery mildew *Blumeria graminis* f. sp. *hordei* (*Bgh*) were then used as templates for iterative homology searches in the same haustorial cDNA library (Pedersen et al., 2012; Weßling et al., 2012). These iterations identified two and ten additional *OECs*, respectively, yielding a total of 115 *OECs*. Sequence relatedness among *Gor* effectors was usually low (Figure 1B). Sequences with similarity to *OECs* were rare in the *Bgh* genome but frequent in the genome of the pea powdery mildew *Erysiphe pisi* (Figure 1B). This pattern is consistent with the different evolutionary distances between *Gor* and the two other powdery mildew species and suggests that conserved effectors may constitute elements of a putative powdery mildew core effector set. We subsequently cloned the open reading frames (ORFs) of mature OECs without signal peptides into Gateway Entry vectors and verified the identity of 84 full-length *OECs* clones (73% success rate) (Table S1 available online).

Systematic Host-Protein Interactome Mapping Using the *G. orontii* Effector Candidates

We defined protein-protein interactions between 69 OECs and 12,000 *Arabidopsis* proteins encoded by sequence-verified ORFs (12k_space) (15 of the 84 OECs autoactivated and were not screened). A subset of 8,000 ORFs (8k_space) was previously used to generate the *Arabidopsis* Interactome 1 (AI-1) and the Plant-Pathogen Immune Network 1 (PPIN-1) (Consortium, 2011; Mukhtar et al., 2011). We used a stringent Y2H mapping pipeline, which yields high-quality data with a low false-discovery rate (Braun, 2012; Dreze et al., 2010) (Figure 1C), to assemble a *Gor* effector-host interactome network (*Gor*_EHIn$_{12k}$) (Figure S1; Table S1). The subset of interactions of OECs with host-proteins within the previously screened 8k_space is denoted *Gor*_EHIn$_{8k}$ (Figure S1). In *Gor*_EHIn$_{12k}$, we found, on average, 2.3 interaction partners for positive OECs (Figure 1E); 38 OECs yielded no interactor. Conversely, 16 host proteins interacted with multiple, typically phylogenetically unrelated, OECs (Figures 1D and S1C). This new data set allowed us to consider whether the host interactors of OECs included previously observed interactors of oomycete and bacterial effectors and whether the convergence previously observed for *Psy* and *Hpa* extended to the *Gor* effector host network.

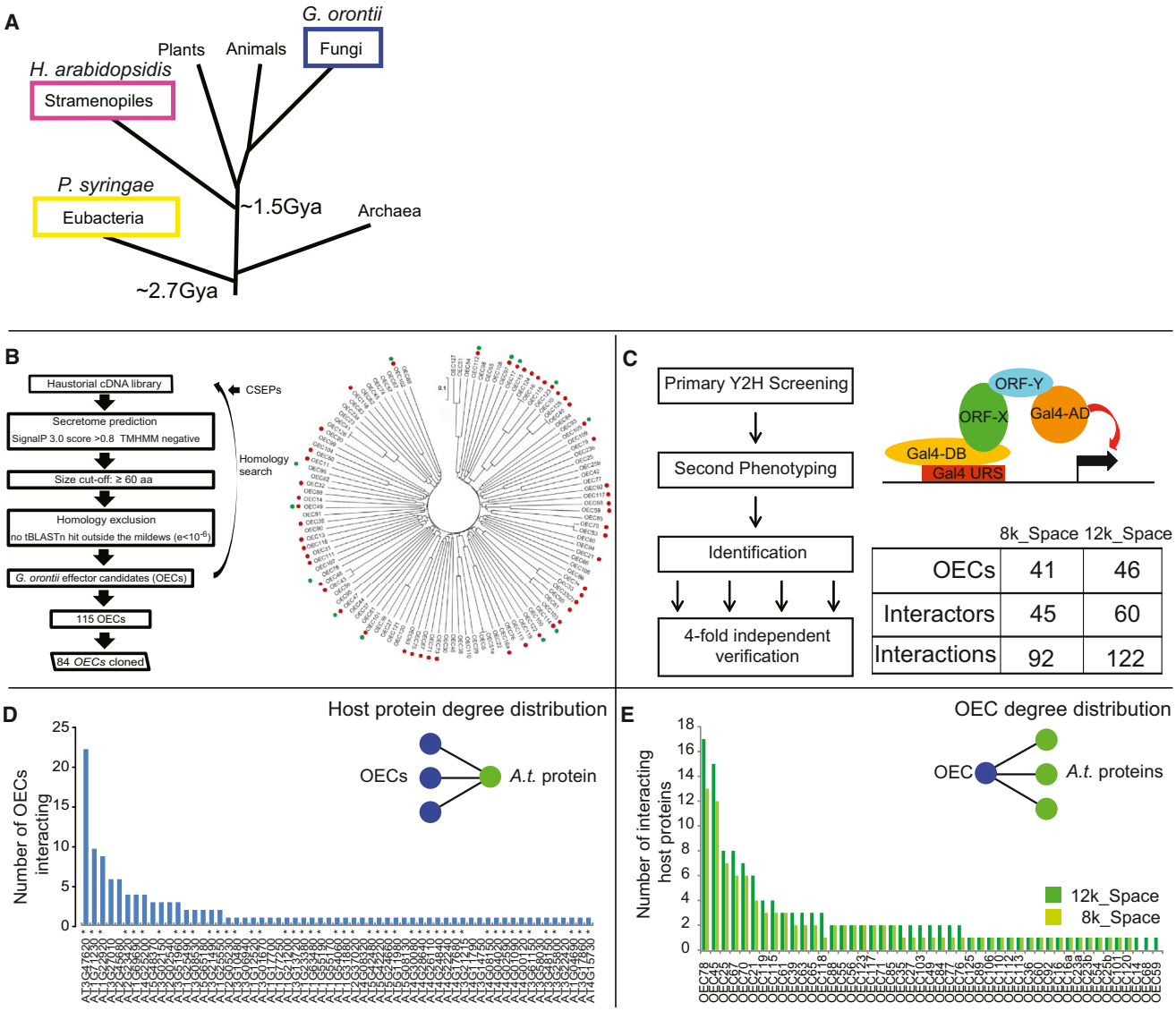

Figure 1. *Gor* Effector Identification and Interactome Mapping

(A) *Golovinomyces orontii* is a pathogenic ascomycete that diverged approximately 2.7 and 1.5 billion years ago (Gya), respectively, from the other *Arabidopsis* pathogens (Kemen and Jones, 2012; Markow, 2005).

(B) Effector identification pipeline and family relationships of identified and cloned *OECs* and the presence of homologs in the powdery mildews *Blumeria graminis* f. sp. *hordei* (green dots) and *Erysiphe pisi* (red dots).

(C) Our Y2H pipeline consists of three interrogation steps: screening, phenotyping, and 4-fold verification, resulting in the indicated number of interactions.

(D) Degree distribution of *Arabidopsis* proteins interacting with OECs. Asterisks indicate 8k_space proteins.

(E) Degree distribution of OECs interacting with *Arabidopsis* proteins in the 8k_space (light green) and 12K_space (dark green). See also Figure S1 and Table S1.

Integrated Network Map Reveals Interspecies Effector Convergence onto Shared Host Proteins

The interactions of effectors from all three pathogens (*Gor*, *Hpa*, and *Psy*) with host proteins were integrated with interactions among host proteins from AI-1, PPIN-1, and the literature to yield a comprehensive Plant-Pathogen Immune Network 2 (PPIN-2) (Figure S2; Table S1). To generate a network produced with identical experimental parameters, effector interactions with the *Arabidopsis* 8k_space proteins were extracted and integrated with their mutual interactions from the systematic AI-1_{MAIN} data set to yield PPIN-2_{8k_sys} (Figure 2A; Table S1). PPIN-2_{8k_sys} consists of 178 *Arabidopsis* host proteins and 123 effectors connected by 421 effector host-protein interactions and 162 interactions among host proteins (Figure S1B). PPIN-2_{8k_sys} was used for all subsequent statistical analyses unless otherwise noted. An overview describing the different data sets is provided in Figure S1.

One large cluster was apparent within PPIN-2_{8k_sys} in which 88 of the 178 effector-interactors (49%) are connected to each other by AI-1_{MAIN} interactions (Figure 2A). Eighty-six effector-interacting host proteins did not interact with any other effector-interactor in AI-1_{MAIN}, although some were connected

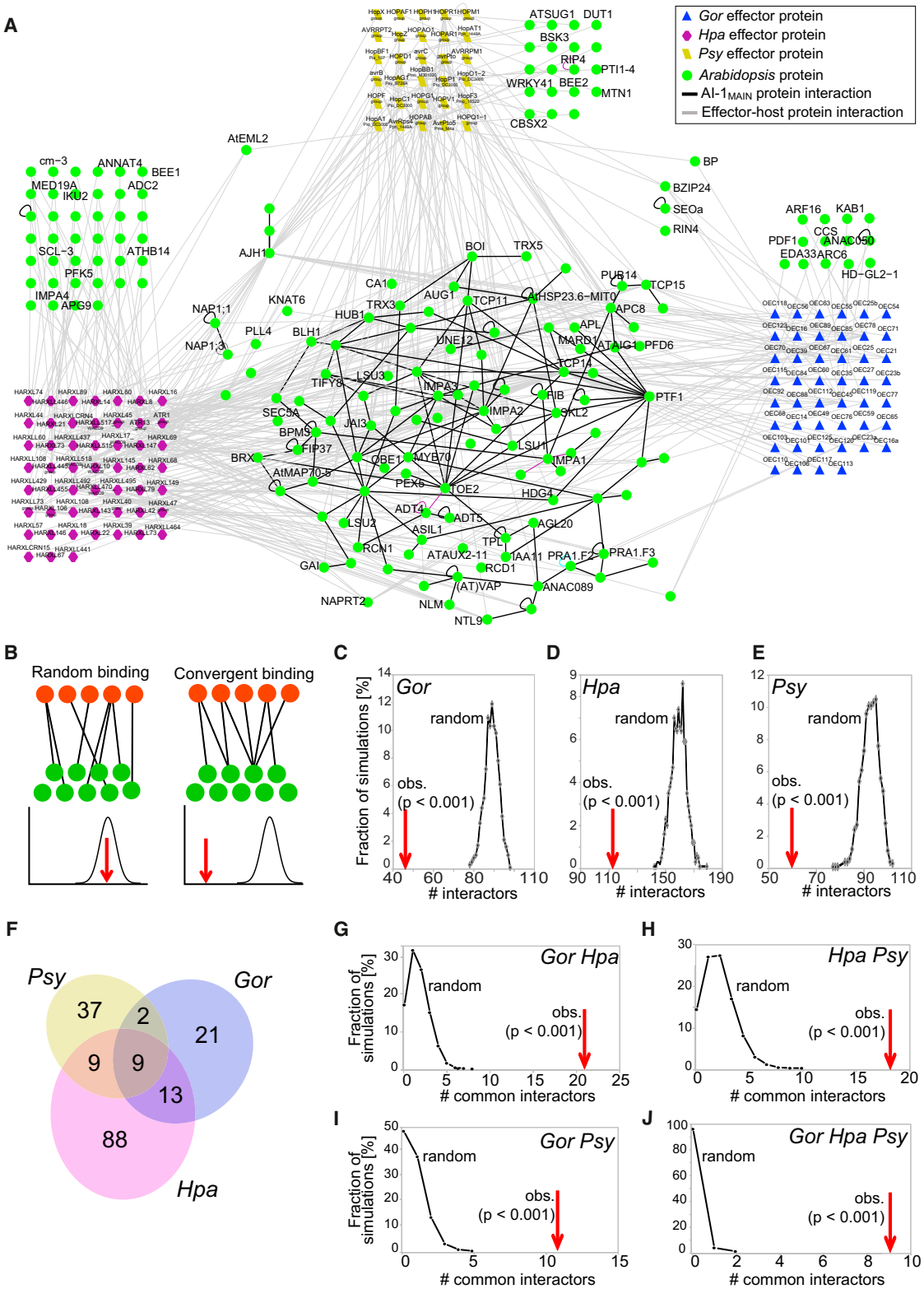

Figure 2. Network Integration

(A) The integrated PPIN-2_{8k_sys} network of host proteins interacting with *Gor*, *Hpa*, and *Psy* effectors and physical interactions among host proteins derived from AI-1_{MAIN} in the 8k_space.

(B) Random and convergent interaction of *Arabidopsis* proteins (green) with effectors (red) can be distinguished by degree-preserving random network rewiring and simulation.

(legend continued on next page)

by interactions from other data sets (e.g., PPIN-1 or literature data) (Figure S2A). Degree-preserving random network rewiring revealed that the effector-interactors were less connected to each other in AI-1_{MAIN} than expected by chance (exp. $p < 0.001$; Figure S2B). This finding may indicate that effectors collectively target different parts of the overall network rather than a functionally coherent subnetwork.

Gene ontology (GO) enrichment analysis on TAIR10 annotations of effector targets returned mostly high-level categories of regulatory processes (Table S2), including defense signaling, potentially due to our previous data being incorporated into the TAIR annotation. We focused on specific, and hence more informative, GO terms that annotate less than 100 genes in AI-1_{MAIN} and found terms related to development (e.g., floral organ development), auxin- and salicylic-acid-mediated signaling, and others (p value 0.005; Table S2). Both of these phytohormones play important roles in plant pathogen interactions (Robert-Seilaniantz et al., 2011). The functional categories are consistent with analysis of specific bacterial effectors and their targets (Deslandes and Rivas, 2012; Win et al., 2012).

To evaluate whether the apparent OEC convergence onto common host proteins (Figure 1D) was significant, we simulated OECs randomly interacting with AI-1_{MAIN} proteins. The frequency distribution of the randomly observed values obtained in these simulations was used to calculate an experimental p value for OEC interactions with host proteins (Figure 2B). We performed 10,000 simulations with all proteins in the AI-1_{MAIN} network represented according to their degree in AI-1_{MAIN}. The mean random expectation of more than 80 OEC-interacting proteins is significantly higher than the experimentally observed value of 45 *Arabidopsis* proteins interacting with OECs in $EHIn_{8k\_sys}$ (Figure 2C; exp. p value < 0.0001). Thus, OEC effectors converge onto a small set of host proteins. We refer to the convergence of effectors from a single pathogen species onto common host proteins as "intraspecies convergence." Applying this analysis to *Hpa* and *Psy* effectors revealed the same striking and significant intraspecies convergence as observed for OECs (Figures 2D and 2E; exp. p value < 0.0001). Thus, effectors of pathogens from diverse kingdoms exhibit intraspecies convergence onto host proteins.

We previously observed convergence of the combined *Psy* and *Hpa* effector sets onto common host proteins ("interspecies convergence"), several of which were hubs (highly interconnected host proteins) (Mukhtar et al., 2011). The *Gor*_EHIn data enabled us to extend the finding of convergence to a divergent fungal pathogen. Effectors from the three pathogens exhibited remarkable overlap with regard to shared host-interacting proteins within $EHIn_{8k\_sys}$; this included 24 host proteins interacting with effectors from two pathogens and nine host proteins interacting with effectors from all three (Figure 2F). We performed simulations for all pairwise, and the three-fold, combinations of the three pathogens. In each case, the experimentally observed overlap was significantly higher than expected by chance (Figures 2G–2H; exp. p value < 0.0001).

Thus, we observed significant intraspecies and interspecies convergence of effectors from three evolutionarily highly diverse (hemi-)biotrophic pathogens. This strongly suggests that the convergence is the product of natural selection and that the respective host proteins are functionally relevant to the pathogen.

Genetic Support for Effector-Interactors: Altered Infection Phenotypes

We tested the functional relevance of 124 effector-interacting host proteins in PPIN-2_{8k_sys} using available transfer DNA (T-DNA) insertion mutants (Alonso and Ecker, 2006). We focused on exon insertions early in genes and tested independent alleles when available (Table S3). We confirmed by PCR both T-DNA insertion into the gene of interest and homozygosity for a total of 179 T-DNA lines. We did not confirm each line as an mRNA null, leaving the formal possibility of phenotypic false negatives. These validated mutants were phenotyped using the *Gor* isolate MPIPZ (Spanu et al., 2010), which is virulent on the Col-0 genetic background of the mutants (Micali et al., 2008; Weßling et al., 2012); *Psy* strain *Pto* DC3000, also virulent on Col-0; and three *Hpa* isolates: Emwa1, Emoy2, and Noco2. The *Hpa* isolates Emwa1 and Emoy2 are avirulent on Col-0 due to RPP4-mediated recognition, whereas *Hpa* Noco2 is virulent on Col-0 (van der Biezen et al., 2002). The *Hpa* isolates were selected to detect both enhanced disease susceptibility (*eds*) and enhanced disease resistance (*edr*) phenotypes.

At least one altered infection phenotype was detected for 63 of the 124 tested effector-interactors (51% validation rate) (Figures 3A, 3B, and S3; Table S3). The 63 interactors with infection phenotypes will be referred to as effector *targets*. Of these, 25 (40%) demonstrated exclusively *eds* phenotypes upon pathogen challenge, indicating that the corresponding wild-type proteins function in immune responses. Mutants for 21 targets (33%) exhibited exclusively *edr* phenotypes upon pathogen challenge, most pronounced in response to the virulent *Hpa* isolate Noco2. These host proteins may facilitate pathogen sustenance in the host. Alternatively, they may repress an activator of immune signaling, a function possibly stabilized by the interacting virulence effectors; thus, in the absence of the putative negative regulator, effector action is neutralized and host resistance increases. We noted divergent disease phenotypes for 17 (27%) effector targets; these are cases where mutants exhibited an *edr* phenotype with one pathogen or *Hpa* isolate and an *eds*

(C) Random interactors observed in degree-preserving network rewiring simulations of *Gor* effector-host protein interactions versus observed value.
(D) As in (C), but for *Hpa* effector-target interactions.
(E) As in (C), but for *Psy* effector-host protein interactions.
(F) Venn diagram showing observed overlap between effector-interactors from the three pathogens.
(G) Simulated random and observed overlap between *Gor* and *Hpa* effector-interactors.
(H) As in (G), but between *Hpa* and *Psy* effector-interactors.
(I) As in (G), but between *Gor* and *Psy* effector-interactors.
(J) As in (G), but between *Gor*, *Hpa*, and *Psy* effector-interactors. In (C)–(E) and (G)–(J), random simulations are shown by black lines and observed values are highlighted by red arrows. See also Figure S2 and Table S1.

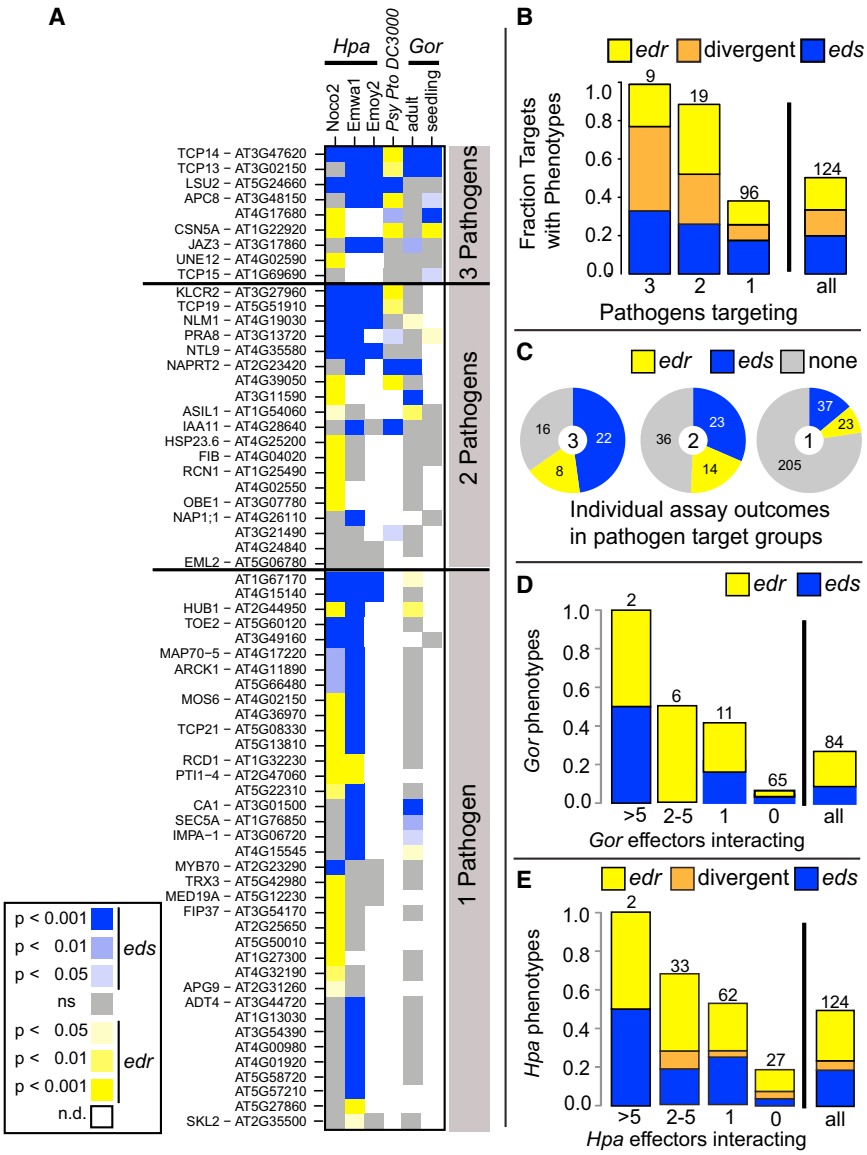

Figure 3. Phenotypic Characterization of Effector-Interactor Mutants

(A) Heatmap summarizing the outcome of phenotypic analyses of mutants in genes encoding the indicated effector-interactors in infection assays with the noted pathogens and developmental stages. Host proteins are sorted by the number of pathogens interacting with them, then by number of observed phenotypes and performed assays. Mutant lines for 59 proteins interacting with effectors from a single pathogen did not show any disease phenotype and are not shown. Refer to Table S3 for raw data for all phenotyped loci and Figure S3 for complete results for all tested lines.

(B) Fraction of mutant lines for proteins interacting with effectors from the indicated number of pathogens that exhibited an *edr*, *eds*, or divergent phenotypes across the assays.

(C) Pie chart representation of the phenotype density; the number of observed phenotypes relative to individual assays performed for that group. Each pie displays data for proteins that interacted with effectors from the number of pathogens given in the center.

(D) Fraction of mutant lines for proteins targeted by the indicated number of *Gor* effectors for which *edr* or *eds* phenotypes were observed. Numbers above bars indicate the number of targets in that class.

(E) As in (D), but for proteins targeted by the indicated number of *Hpa* effectors for which *edr* or *eds* phenotypes were observed. Numbers above bars indicate the number of effector-interactors in the class.

phenotype with a second pathogen or a different *Hpa* isolate, as described in Pieterse et al., (2012). Their existence suggests that these host proteins may have disease-specific functions. The TCP transcription factors TCP13, TCP14, and TCP19, whose mutants exhibited *eds* phenotypes with the biotrophic pathogens *Hpa* and *Gor*, but *edr* phenotypes with the hemibiotrophic *Psy*, are particularly interesting in this context.

Effector Convergence Correlates with Altered Infection Phenotypes

The nonrandom nature of effector-host protein connectivity suggested that the network topology of the plant immune system is the product of natural selection and, consequently, that the convergence we observed is biologically meaningful. We explored whether a relationship exists between intraspecies and interspecies effector convergence and altered pathogen infection phenotypes. A host protein was considered a point of intraspecies convergence when at least two effectors from the same pathogen interacted with it and an object of interspecies convergence when effectors from different pathogens interacted with it.

Effector-interactors were binned by whether they interacted with effectors from three, two, or one pathogen(s) (Figure 2F). The rate of altered infection-related phenotypes was evaluated for each bin and compared to the overall rate ("all" column) (Figure 3B). We noted a positive correlation between the degree of interspecies convergence and the probability of observing an infection phenotype in that bin (Figure 3B). To exclude that our observation was due to deeper phenotypic interrogation of the most highly targeted proteins, we also calculated the phenotype density for proteins interacting with effectors from three, two, or one pathogen as the fraction of assays (individual squares in Figure 3B) in which an *edr* or *eds* phenotype was observed divided by the total number of assays performed in this group. This analysis confirmed the correlation between convergence and phenotypic relevance of the targeted host protein (Figure 3C).

We then evaluated the phenotypic relevance of genes encoding host proteins that are objects of intraspecies convergence (Figures 2C–2E). We binned host proteins according to the number of effectors from each pathogen interacting with them and evaluated how often an altered immunity phenotype could be observed with the respective pathogen. We found *edr* or *eds*

phenotypes for all mutants in genes encoding the proteins targeted by more than five *Gor* or *Hpa* effectors (Figures 3D and 3E). The fraction of phenotypically validated host targets decreased proportional to the degree at which effectors are connected to the respective plant proteins (Figures 3D and 3E). Thus, the extent of intraspecies effector convergence onto host targets is also directly correlated to the functional relevance of the targeted proteins.

We wondered whether the host proteins that interact with effectors from multiple pathogens were also targeted repeatedly by the suite of effectors from any individual pathogen. All nine *Arabidopsis* proteins targeted by effectors from all three pathogens are also intraspecies convergence points for at least one pathogen (Figure S3). Furthermore, 16 of 23 proteins targeted by effectors from two pathogens are also points of intraspecies convergence. Thus, the most commonly targeted *Arabidopsis* proteins are objects of both intraspecies and interspecies effector convergence (Fisher's exact test, $p < 0.001$).

Effector convergence is exemplified by TCP14, a member of a large family of transcriptional regulators typically recognized to function in plant development (Martín-Trillo and Cubas, 2010). TCP14 was the most targeted host protein, interacting with 23 distinct OECs, 25 *Hpa* effectors, and four *Psy* effectors and exhibiting disease phenotypes in all assays (Figure 3A). The related family members TCP13, TCP15, and TCP19 were also targeted multiple times by effectors from at least two pathogens and exhibited altered infection phenotypes. These findings suggest an important and possibly universal role of this class of TFs during infection, consistent with their emerging role as targets of phytoplasma effectors (Sugio et al., 2011) and the recent demonstration of their importance in plant immunity (Kim et al., 2014).

Effectors Colocalize with TCP14 In Planta

To independently validate the convergence concept using cell biological methods, we tested TCP14 for colocalization with 11 of the 25 interacting *Hpa* effectors, focusing on those effectors demonstrated to localize to the nucleus (Caillaud et al., 2012), 19 of the 23 *Gor* effectors not previously localized, and three of four *Psy* effectors (Table S4).

TCP14 localized to subnuclear foci in transgenic *Arabidopsis* plants expressing a functional TCP14-YFP fusion (Figure S4). We used this knowledge to develop a transient overexpression assay platform in *Nicotiana benthamiana* where TCP14-RFP was also localized to subnuclear foci (Figure 4A). Under these conditions, TCP14-RFP did not colocalize with a wide set of controls with which it did not interact in Y2H: free YFP (Figure 4B), representative effectors (HopBC1, HaRxL62, and OEC56), an unrelated TF (bZIP5), or an unrelated, subnuclear body-localized protein (PhyB) (Chen et al., 2005) (Figure S4). We then demonstrated that TCP14 can relocalize into subnuclear foci 64% and 74% of the tested *Hpa* and *Gor* effectors, respectively, and one of three *Psy* effectors (Figures 4C and S4). Thus, the majority (67%) of tested interactions between effectors and TCP14 were validated by relocalization in vivo (Table S4). We confirmed these findings via coimmunoprecipitation for single effectors from each pathogen (Figure 4D). We thus validated in planta the majority of effector interactions with the most heavily targeted host protein, TCP14, consistent with our claim that the observed convergence onto the plant protein is not an artifact.

Proteins Interacting with Common Effector Targets Are Likely under Positive Selection

We sought evidence for the evolutionary relevance of our effector targets from population genomics. We used the complete genomes of 80 accessions sequenced in the context of the 1001 Genomes project and mapped on the Col-0 reference genome (Cao et al., 2011). These were collected in eight regions distributed over Europe and Asia, where *Arabidopsis* naturally occurs, and thus provide a large spatial and phylogenetic sample of genotypes adapted to different environments (http://1001genomes.org/data/). For all proteins in AI-1_{MAIN}, we calculated Tajima's D (D_T) and Watterson's estimator θ (θ_W) to assess the allele frequency deviation from neutrality and scaled mutation rate, respectively (Tajima, 1989; Watterson, 1975) (Table S5). As the two statistics lead to different ordered gene rankings, we also built a consensus ranking based on the relative positions of each gene in the two ranked lists (Dθ-ranking). In addition, we constructed consensus protein sequences from 81 *Arabidopsis* accessions (80 plus the Col-0 reference) by majority voting (S.A., K.C.B., K.F.X.M., and P.B., unpublished data) and used this resource to identify SNPs that give rise to altered amino acid sequences (amino acid polymorphisms [AAPs]) in the 2,653 AI-1_{MAIN} proteins (Table S5).

We asked whether the direct effector-interactors exhibit evidence for balancing selection, as indicated by positive D_T values (Figure S5A). No significant deviation from random expectation could be detected for any of four effector-interactor groups: (i) all effector-interactors, (ii) interactors of effectors from two or three pathogens, (iii) interactors of effectors from three pathogens, and (iv) phenotypically supported effector-interactors (Figure S5A). For three of the four groups, the mean of D_T for effector-interactors is lower than that of random controls, whereas for the group targeted by three pathogens the mean is slightly higher.

The lack of a strong signal can likely be explained by our previous observation that many effector targets are central proteins in the network, which likely cannot tolerate much variation without adverse effects on protein function. We therefore asked whether instead there might be evidence for the selective pressure imposed by pathogens in the network neighborhood of the effector-interactors. To this end, we explored whether the AI-1_{MAIN} interaction partners of effector-interactors are subject to balancing selection, but no such evidence could be detected for any of the effector-interactor groups ($p = 0.51–0.94$) (Figure S5B). It is possible that a majority of interacting proteins mediating nonimmune functions may mask any potential signal from the few interacting proteins involved in immune functions. We therefore adopted an inverse approach and investigated whether effector-interactors are preferential interaction partners of proteins encoded by genes under balancing selection. For each cutoff of the top-ranking genes in the combined Dθ-ranked list, we counted the cumulative number of interacting effector-interactors in AI-1_{MAIN} (red dots) separately for each of the four effector groups noted above (Figure 5). To estimate the specificity of the observations in the context of the experimentally derived network structure, we performed rewiring controls of AI-1_{MAIN} and counted randomly interacting effector-interactors for the same top Dθ-ranking proteins (Figure 5A). The number of interacting effector-interactors in the real AI-1_{MAIN} network is always significantly higher than random across a range of cutoffs, demonstrating a preferential interaction of proteins

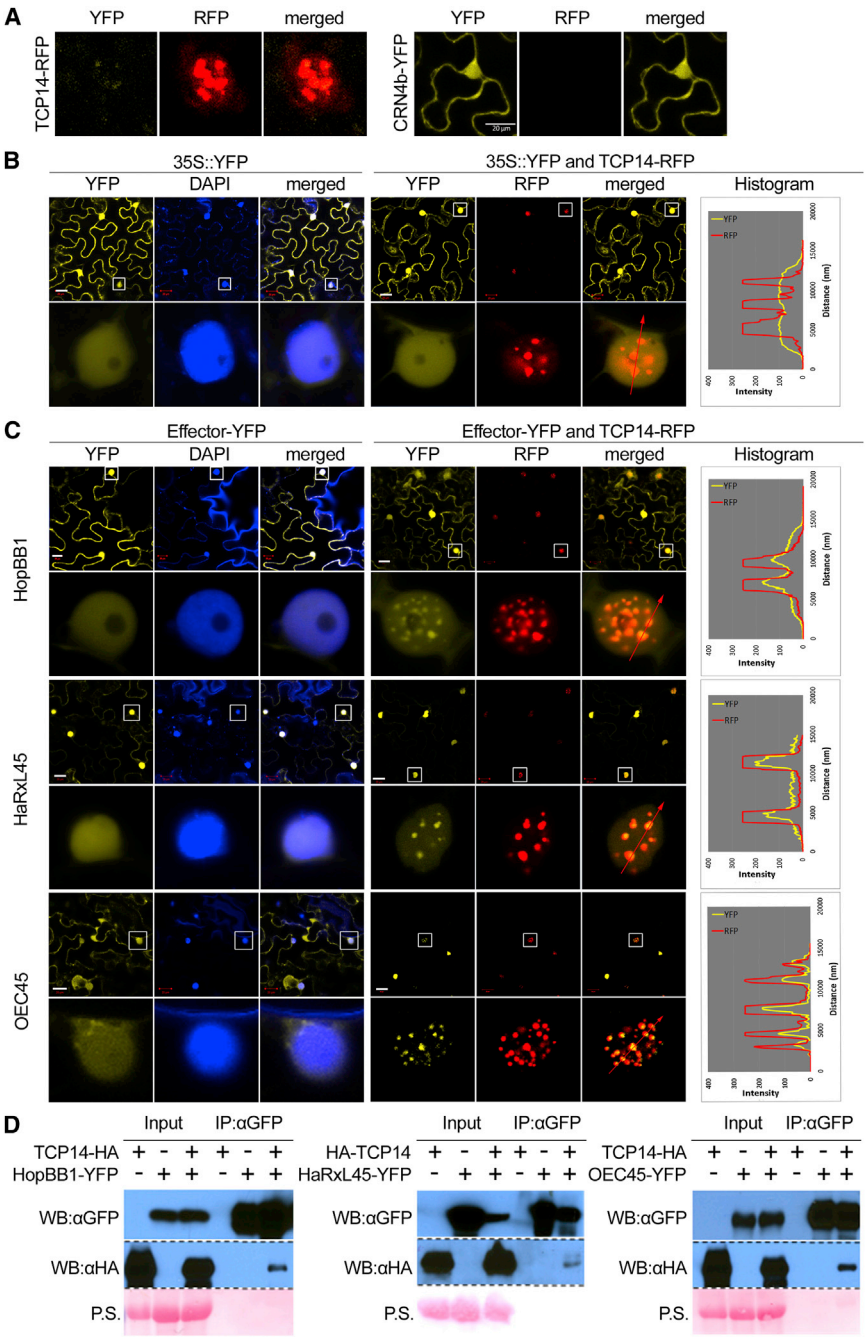

Figure 4. TCP14 Relocalizes Effectors to Subnuclear Foci

(A) Technical control demonstrating that YFP and RFP channels do not leak into each other. The images show localization of TCP14-RFP and CRN4b-YFP; image data for YFP and RFP channels were collected for both. The same settings were then applied to all assays below. Note that TCP14-YFP forms subnuclear foci.

(B and C) The lower panel exhibits an enlarged view of a representative nucleus boxed in the upper panel. The histogram illustrates the intensity of fluorescent signal across the path indicated by the red arrow. All confocal pictures were taken 40–48 hr after infiltration of Agrobacterium strains expressing the different fluorophore-tagged proteins.

(B) Negative control: TCP14 does not relocalize YFP.

(C) TCP14 relocalizes effectors from *Psy* (HopBB1), *Hpa* (HaRxL45) and *Gor* (OEC45) to subnuclear foci.

(D) TCP14 is coimmunoprecipitated by HopBB1, HaRxL45, and OEC45. All proteins were expressed from the CaMV 35S promoter in *N. benthamiana* leaves. "P.S" denotes Ponceau S staining. The 20 μM size bars ([A], right; [B] and [C] top rows) mark the first of three images from the same field. The length of a side of the nuclear images ([A], left; [B] and [C] bottom rows) is 20 μM. See also Figure S4 and Table S4.

The network of four of the top Dθ-ranking five proteins further shows that even the two interaction partners that are not effector-interactors are members of a common subnetwork by virtue of multiple interactions with variable proteins and effector-interactors (Figure 5F). The underlying biological reasons of how the increased genetic variation is beneficial in the evolutionary battle remain to be elucidated. A GO enrichment analysis of the top Dθ-ranking genes did not yield conclusive results, though, partly because many of these genes have not yet been characterized.

The evidence for preferential interaction of proteins encoded by genes under balancing selection with effector-interactors contrasts with the conservation of effector-interactors themselves, which show signs of purifying selection (Figure 5F). Together, these data demonstrate that at least a subset of proteins targeted by multiple evolutionary distant pathogens are under purifying selection, and in such instances, variation at the level of neighbors in the protein interaction network becomes a substrate for balancing selection.

encoded by genes under balancing selection with our effector-interactors. These findings are supported by similar results obtained with an AAP-based ranking, although with slightly different top-ranking proteins. These polymorphic proteins show the greatest signal with effector-interactors targeted by effectors from three pathogens. The protein with the greatest number of AAPs is an intracellular TIR-NLR type immune receptor (AT1G31540), which interacts with TCP14 and is characterized by the third-highest-ranking θ value (0.021) among all $AI\text{-}1_{MAIN}$ proteins. Previously, TIR-NLR was identified as the dominant *RAC1* gene, mediating resistance to *Albugo candida* in the Ksk-1 accession (Borhan et al., 2004).

DISCUSSION

We identified interactions between candidate virulence effector proteins from the obligate biotrophic powdery mildew fungus

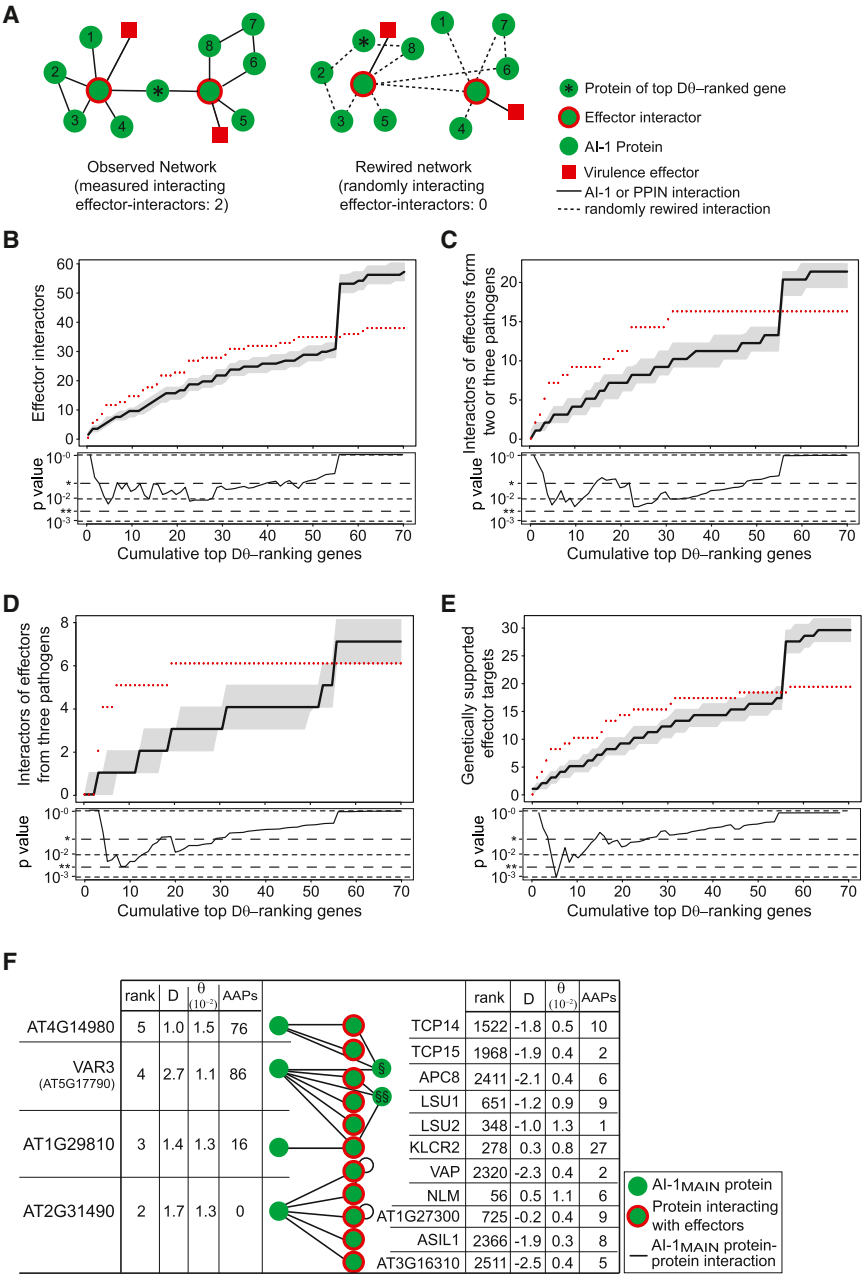

Figure 5. Proteins with High Natural Genetic Variation Interact with Effector-Interactors

(A) Schematic illustration of the analysis in (B)–(E): in the AI-1_{MAIN} network (left) the effector-interactors directly interacting with top Dθ-ranking gene products are counted and compared to the distribution of counts observed in 1,000 randomly rewired networks (single example shown). Effectors are shown for illustration only and not included in the analysis.

(B) Analysis as described in (A). Plotted along the y axis are cumulative counts of effector-interactors interacting with proteins encoded by the top Dθ-ranking x genes. Data from AI-1_{MAIN} are shown as red dots; the black line shows the median of 1,000 randomly rewired networks; gray shaded areas show the 25th and 75th percentiles of values from rewiring controls. The lower panel shows the corresponding experimental p values (* 0.05; ** 0.005). The steep rise in the simulations at x = 56 is caused by a high-degree protein (NLM1, AT4G19030) at that position; the many rewired interactions for this protein increase the count of random interactors in all categories.

(C) As in (B), but counting proteins interacting with effectors from two or three pathogens.

(D) As in (B), but counting proteins interacting with effectors from three pathogens.

(E) As in (B), but counting proteins whose mutation caused altered immune phenotypes.

(F) Among the 13 interaction partners of the five most selected proteins are eleven effector-interactors, including the five most targeted proteins. The tables show for all top Dθ-ranking proteins and effector-interactors the relative combined rank, D_T, θ_W, and the count of AAPs. The non-effector-interactor interactors of the variable proteins are § AT1G51580 and §§ ZPF7. See also Figure S5 and Table S5.

Golovinomyces orontii and proteins from its host, *Arabidopsis*. We added these to previously defined interactions between the same set of host proteins and effector suites from two pathogens derived from different kingdoms. Analysis of the combined data allowed us to significantly extend our previously defined principles of how plant pathogens have independently evolved effectors to converge onto a limited, shared set of host proteins. Our main conclusions will propel future hypothesis testing, ultimately resulting in the definition of key plant machinery modulated by diverse pathogens to increase their fitness during infection.

Our identification and analysis of *Gor* candidate effectors serves two functions. First, it paves the way for mechanistic studies of single effectors and elucidation of the infection strategies of fungal pathogens in general. Incidentally, several OECs that interact with functionally relevant targets, such as the highly connected OEC78 or the less connected OEC49 and OEC101, have homologs in *Bgh* and *Erysiphe pisi* and may be part of a putative powdery mildew core effector set (Figure 1B). Unfortunately, it was not possible to clearly differentiate host proteins as being targeted by core or noncore proteins, which prevented a deeper characterization.

Second, our systematic and unbiased identification of *Gor* effector interactors enabled combined analyses of host-pathogen interaction networks when integrated with our previous data for *Hpa* and *Psy* (Mukhtar et al., 2011). The result is a map of *Arabidopsis* proteins interacting with effectors from three destructive pathogen lineages: bacteria, oomycetes, and fungi (Figure 2A; Table S1). We demonstrate that most of the host interactors are genuine targets, in the sense that loss-of-function results in altered host immune system function (Figures 3A, 3B, and S3; Table S3). In the combined PPIN-2 network, we also significantly expand our previous evidence for interspecies effector convergence (Mukhtar et al., 2011).

We discovered evidence for combined intraspecies convergence by effectors of each of the three pathogens (Figure 2F). Our data indicate that effector-target convergence evolved independently in all kingdoms of life. Thus, convergence per se may be an important, if not necessary, feature of host-pathogen interactions. The mechanistic and evolutionary principle for this convergence is speculation, but it may suggest that successful biotrophic pathogens need to manipulate a largely shared set of physiological host networks and proteins. They may achieve this, in the face of receptor-based host immune surveillance, by homology-independent functional redundancy that uses different effectors to modulate different nodes in a common set of subnetworks, as suggested by our findings (Figure S1C). Additional pathogenicity strategies evolved by other biotrophic or nonbiotrophic pathogens may drive the evolution of idiosyncratic pathogen species-specific host targets or of completely new host machinery that is required to support lifestyles beyond those of the pathogens whose effector suites we have surveyed.

Genome sequencing of pathogenic bacterial strains revealed that effector complements are only marginally overlapping, even between strains that otherwise exhibit very high genomic sequence identity (97%) (Baltrus et al., 2011). Likewise, genome sequencing in a variety of oomycete lineages reveals diverse expansion and contraction in effector families (Pais et al., 2013; Stergiopoulos et al., 2012). Thus, the observed intraspecies convergence of effectors supports our suggestion of functional redundancy mediated by different effectors to maintain host protein targeting. The effector complement would thus be buffered against loss or rapid selection against specific effectors due to host recognition. Importantly, the plant immune system can blunt effector evolution by detecting effector-dependent host target modifications. It is much more efficient to guard a limited number of important host targets than to evolve receptors for each effector (Jones and Dangl, 2006), especially in cases where both the effector and the host receptor are under frequency-dependent balancing selection (Van der Hoorn et al., 2002). Our observations that in our systematic network (1) effectors converge onto limited number of targets and (2) a large fraction of targets, in turn, interact with highly polymorphic proteins that are under balancing selection across the *Arabidopsis* population support this notion. Alternative explanations for effector convergence include the sequential delivery of effectors targeting the same host-protein, but at different time points in the course of host colonization and/or cooperativity of effectors that might act together to modify host protein functions. Intriguingly, most *Hpa* effectors, when delivered via bacteria, conferred enhanced virulence on only a subset of *Arabidopsis* accessions in *Psy* infection assays, indicating variation between accessions in the susceptibility to effector manipulation (Fabro et al., 2011).

Integrating these network concepts with our extensive reverse genetic data, we demonstrate that effector convergences strongly correlate with mutant infection phenotypes (Figures 3B–3E). Our genetic data convincingly reinforce our interpretation that network convergence is due to selection of effector interactions with host proteins. Our mutant phenotyping results also show that most host targets of multiple pathogens have previously unknown plant immune system functions. This conclusion is substantiated by the fact that effector-interactors are also preferential interaction partners of intracellular NLR receptors, likely reflecting guarding of these virulence targets by the plant immune system (Mukhtar et al., 2011).

To demonstrate that interactions between effectors and highly targeted host-proteins can occur in planta, we investigated TCP14, the host protein most commonly targeted by effectors. These experiments demonstrated that the majority of tested effectors that interact with TCP14 in Y2H are relocalized in the nucleus to characteristic TCP14 subnuclear foci (Figure 4C and S4; Table S4). The function of the TCP14 foci and the function(s) of specific effectors within them are now the object of active investigation. Together with extended genetic support for TCP14 function in response to infection, our findings strengthen the hypothesis that the majority of effector-TCP14 interactions reflect genuine protein-protein interactions that function during infections by diverse pathogens.

Plants and microbial pathogens are engaged in a constant evolutionary battle in which pathogens can expand their suites of effectors via horizontal gene transfer, or evolution of new alleles of existing effectors, driving selection in plants to respond accordingly. Each successful evolutionary step in the plant can be overcome by subsequent modification of pathogen effector deployment. Yet both pathogen virulence and plant immune function have fitness costs that can drive the arms race into balanced trench warfare (Holub, 2001). The current shape of the plant immune system is a consequence of these counteracting forces. The network we define here is uniquely well supported by broad mutant phenotype analysis and cell biological investigation.

EXPERIMENTAL PROCEDURES

Effector Prediction and Cloning

Secreted proteins were identified in a cDNA library from isolated haustoria by employing SignalP3.0 at a HMM threshold of 0.8 and the TMHMM algorithm (http://www.cbs.dtu.dk/services/TMHMM) (Bendtsen et al., 2004). A size cut-off of $\geq$60 amino acids was applied. The absence of homologs in unrelated species was confirmed by BLAST. In a second prediction round, 491 *Bgh* Candidates for Secreted Effector Proteins (Pedersen et al., 2012) and effector candidates from the first round were used as templates for tBLASTn and BLASTp analyses of the haustorial cDNA library. Putative homologs of predicted effectors were then subjected to SignalP3.0 and TMHMM analysis, and the absence of homologs in unrelated species was confirmed to prevent false positives. Finally, the conservation of OECs in the genomes of *Bgh* and *E. pisi* was queried by tBLASTn. A multiple sequence alignment of the *OECs* was generated using ClustalW (http://www.ebi.ac.uk/Tools/msa/clustalw2/) and imported into MEGA5 (Tamura et al., 2011). The phylogeny was computed with default parameters using the Neighbor-joining algorithm and a p-distance model for amino acid substitutions. For *OEC* cloning, primers spanning the mature protein (without signal peptide) were generated and used for PCR from a mix of cDNA constructed from plant material at 1, 3, 5, and 10 dpi with *G. orontii* using a proof-reading polymerase.

Y2H Analysis

A detailed description of the Y2H pipeline can be found in the Supplemental Information.

Phenotypic Assays

We used *Arabidopsis thaliana* Columbia (Col-0) unless mentioned otherwise. Single mutants for *eds1-2* (Bartsch et al., 2006), *sid2-2* (Dewdney et al., 2000), and *mlo2-6* (Consonni et al., 2006) in the Col-0 genetic background were used as controls for the relevant infection assays. The set of homozygous T-DNA insertion lines is described in Table S3. Pathogen infection assays were performed as described in the Supplemental Experimental Procedures.

Statistical Analysis

Details of the statistical analyses and controls can be found in the Supplemental Information.

Relocalization of Effectors by TCP14

Vector constructs: Coding sequences of *Psy* effectors and coding sequences of *Hpa* and *Gor* effectors lacking the signal peptides were amplified by PCR and then Gateway-cloned into the destination vectors pGWB41, pGWB660, pGWB642, pGWB644, pGWB645, and a modified pMDC7, respectively (Akimoto-Tomiyama et al., 2012; Nakagawa et al., 2007) (Table S4). The plasmids were transformed into the *Agrobacterium tumefaciens* strain GV3101 for transient expression assays in *Nicotiana benthamiana* (see Supplemental Experimental Procedures).

Immunoprecipitation

HA-tagged TCP14 and eYFP-tagged effectors were expressed in *N. benthamiana* under control of the 35S constitutive promoter. The binary vectors used for expression were pGWB614 (for TCP14-HA), pGWB715 (for HA-TCP14), pGWB641 (for HaRxL45-YFP and HopBB1-YFP), and pGWB41 (for OEC45-YFP). Agrobacteria carrying each construct (OD = 0.2) were infiltrated into *N. benthamiana* leaves 24 hr prior to harvesting. Proteins were extracted from 0.5 g of fresh tissue using 2 ml extraction buffer (50 mM HEPES [pH 7.5], 50 mM NaCl, 10 mM EDTA [pH 8.0], 0.5% Triton X-100, 5 mM DTT, and 1x Plant protease inhibitor cocktail from Sigma-Aldrich). Magnetic labeling and separation of tagged proteins was performed using μMACS Epitope Tag Protein Isolation Kit (Miltenyi Biotec). Protein samples were separated by 12% SDS-PAGE. Immunoblots were performed with a 1:1,000 dilution of α-HA (Roche) and 1:1,000 dilution of α-GFP (Roche). Blots were detected by ECL prime (GE Healthcare).

ACCESSION NUMBERS

The GenBank accession numbers for the *G. orontii* effector candidate (*OEC*) sequences reported in this paper are KM220803–KM220886.

All GenBank accession numbers are further listed and associated with the correct OECs in Table S1.

SUPPLEMENTAL INFORMATION

Supplemental Information includes five figures, five tables, and Supplemental Experimental Procedures and can be found with this article online at http://dx.doi.org/10.1016/j.chom.2014.08.004.

AUTHOR CONTRIBUTIONS

OEC identification and cloning: R.W., A.E.S., E.V.L.v.T., and R.P. OEC-At interactome mapping: R.W., L.G., J.R.E., M.V., and P.B. Data integration and convergence statistics: S.A., C.G., K.F.X.M., J.L.D., and P.B. Immune assays (*Hpa*, *Psy*): P.E., K.W., N.M., M.S.M., and J.L.D. Immune assays (*Gor*): R.W., S.H., P.S.-L., and R.P. Phenotype statistics: S.A., P.E., R.W., E.V.L.v.T., and P.B. Colocalization analysis: Y.H., L.Y., and J.L.D. Immunoprecipitations: L.Y., Y.H., and J.L.D. Provision of several *Hpa* effectors: J.D.G.J.; natural variation analysis: S.A., S.R.H., K.C.B., K.F.X.M., D.W., J.L.D., and P.B. Manuscript writing: P.B., P.E., S.A., R.W., and J.L.D. Critical manuscript reading and editing: P.S.-L. and R.P. Conception and design: P.E., R.P., P.B., and J.L.D.

ACKNOWLEDGMENTS

We thank Axel Künstner for helpful discussions about the population genetic analysis. This work was funded by grants to J.L.D. from the National Science Foundation (IOS-1257373), the National Institutes of Health (1RO1 GM107444), the Gordon and Betty Moore Foundation (GBMF3030), and the HHMI. R.W. was supported by a PhD fellowship from the International Max-Planck Research School (IMPRS). J.L.D. is an Investigator of the Howard Hughes Medical Institute. L.Y. was funded in part by the Gordon and Betty Moore Foundation through Grant GBMF 2550.02 to the Life Sciences Research Foundation. Y.H. was supported by a Distinguished Guest Professorship, Eberhard-Karls-Universität, Tübingen, Germany to J.L.D. S.A. and P.B. are supported by the Deutsche Forschungsgemeinschaft (DFG) grant SFB924. R.P. and P.S.-L. were supported by grants from the Max-Planck society. We thank Dr. Meng Chen, Duke University, for 35S:phyB-CFP and useful discussions regarding subnuclear foci.

Received: March 23, 2014
Revised: June 27, 2014
Accepted: August 14, 2014
Published: September 10, 2014

REFERENCES

Akimoto-Tomiyama, C., Furutani, A., Tsuge, S., Washington, E.J., Nishizawa, Y., Minami, E., and Ochiai, H. (2012). XopR, a type III effector secreted by *Xanthomonas oryzae* pv. oryzae, suppresses microbe-associated molecular pattern-triggered immunity in *Arabidopsis thaliana*. Mol. Plant Microbe Interact. *25*, 505–514.

Alonso, J.M., and Ecker, J.R. (2006). Moving forward in reverse: genetic technologies to enable genome-wide phenomic screens in *Arabidopsis*. Nat. Rev. Genet. *7*, 524–536.

Baltrus, D.A., Nishimura, M.T., Romanchuk, A., Chang, J.H., Mukhtar, M.S., Cherkis, K., Roach, J., Grant, S.R., Jones, C.D., and Dangl, J.L. (2011). Dynamic evolution of pathogenicity revealed by sequencing and comparative genomics of 19 *Pseudomonas syrinage* isolates. PLoS Pathog. *7*, e1002132.

Bartsch, M., Gobbato, E., Bednarek, P., Debey, S., Schultze, J.L., Bautor, J., and Parker, J.E. (2006). Salicylic acid-independent ENHANCED DISEASE SUSCEPTIBILITY1 signaling in *Arabidopsis* immunity and cell death is regulated by the monooxygenase *FMO1* and the Nudix hydrolase *NUDT7*. Plant Cell *18*, 1038–1051.

Baxter, L., Tripathy, S., Ishaque, N., Boot, N., Cabral, A., Kemen, E., Thines, M., Ah-Fong, A., Anderson, R., Badejoko, W., et al. (2010). Signatures of adaptation to obligate biotrophy in the *Hyaloperonospora arabidopsidis* genome. Science *330*, 1549–1551.

Bendtsen, J.D., Nielsen, H., von Heijne, G., and Brunak, S. (2004). Improved prediction of signal peptides: SignalP 3.0. J. Mol. Biol. *340*, 783–795.

Borhan, M.H., Holub, E.B., Beynon, J.L., Rozwadowski, K., and Rimmer, S.R. (2004). The *Arabidopsis* TIR-NB-LRR gene *RAC1* confers resistance to *Albugo candida* (white rust) and is dependent on *EDS1* but not *PAD4*. Mol. Plant Microbe Interact. *17*, 711–719.

Braun, P. (2012). Interactome mapping for analysis of complex phenotypes: insights from benchmarking binary interaction assays. Proteomics *12*, 1499–1518.

Caillaud, M.C., Piquerez, S.J., Fabro, G., Steinbrenner, J., Ishaque, N., Beynon, J., and Jones, J.D. (2012). Subcellular localization of the *Hpa* RxLR effector repertoire identifies a tonoplast-associated protein HaRxL17 that confers enhanced plant susceptibility. Plant J. *69*, 252–265.

Cao, J., Schneeberger, K., Ossowski, S., Günther, T., Bender, S., Fitz, J., Koenig, D., Lanz, C., Stegle, O., Lippert, C., et al. (2011). Whole-genome sequencing of multiple *Arabidopsis thaliana* populations. Nat. Genet. *43*, 956–963.

Chen, M., Tao, Y., Lim, J., Shaw, A., and Chory, J. (2005). Regulation of phytochrome B nuclear localization through light-dependent unmasking of nuclear-localization signals. Curr. Biol. *15*, 637–642.

Chisholm, S.T., Coaker, G., Day, B., and Staskawicz, B.J. (2006). Host-microbe interactions: shaping the evolution of the plant immune response. Cell *124*, 803–814.

Consonni, C., Humphry, M.E., Hartmann, H.A., Livaja, M., Durner, J., Westphal, L., Vogel, J., Lipka, V., Kemmerling, B., Schulze-Lefert, P., et al. (2006). Conserved requirement for a plant host cell protein in powdery mildew pathogenesis. Nat. Genet. *38*, 716–720.

Consortium, A.I.M.; Arabidopsis Interactome Mapping Consortium (2011). Evidence for network evolution in an *Arabidopsis* interactome map. Science *333*, 601–607.

Dangl, J.L., Horvath, D.M., and Staskawicz, B.J. (2013). Pivoting the plant immune system from dissection to deployment. Science *341*, 746–751.

Deslandes, L., and Rivas, S. (2012). Catch me if you can: bacterial effectors and plant targets. Trends Plant Sci. *17*, 644–655.

Dewdney, J., Reuber, T.L., Wildermuth, M.C., Devoto, A., Cui, J., Stutius, L.M., Drummond, E.P., and Ausubel, F.M. (2000). Three unique mutants of *Arabidopsis* identify *eds* loci required for limiting growth of a biotrophic fungal pathogen. Plant J. *24*, 205–218.

Dodds, P.N., and Rathjen, J.P. (2010). Plant immunity: towards an integrated view of plant-pathogen interactions. Nat. Rev. Genet. *11*, 539–548.

Dreze, M., Monachello, D., Lurin, C., Cusick, M.E., Hill, D.E., Vidal, M., and Braun, P. (2010). High-quality binary interactome mapping. Methods Enzymol. *470*, 281–315.

Fabro, G., Steinbrenner, J., Coates, M., Ishaque, N., Baxter, L., Studholme, D.J., Körner, E., Allen, R.L., Piquerez, S.J., Rougon-Cardoso, A., et al. (2011). Multiple candidate effectors from the oomycete pathogen *Hyaloperonospora arabidopsidis* suppress host plant immunity. PLoS Pathog. *7*, e1002348.

Feng, F., and Zhou, J.M. (2012). Plant-bacterial pathogen interactions mediated by type III effectors. Curr. Opin. Plant Biol. *15*, 469–476.

Hacquard, S., Kracher, B., Maekawa, T., Vernaldi, S., Schulze-Lefert, P., and Ver Loren van Themaat, E. (2013). Mosaic genome structure of the barley powdery mildew pathogen and conservation of transcriptional programs in divergent hosts. Proc. Natl. Acad. Sci. USA *110*, E2219–E2228.

Holub, E.B. (2001). The arms race is ancient history in *Arabidopsis*, the wildflower. Nat. Rev. Genet. *2*, 516–527.

Jones, J.D., and Dangl, J.L. (2006). The plant immune system. Nature *444*, 323–329.

Kemen, E., and Jones, J.D.G. (2012). Obligate biotroph parasitism: can we link genomes to lifestyles? Trends Plant Sci. *17*, 448–457.

Kim, S.H., Son, G.H., Bhattacharjee, S., Kim, H.J., Nam, J.C., Nguyen, P.D., Hong, J.C., and Gassmann, W. (2014). The Arabidopsis immune adaptor SRFR1 interacts with TCP transcription factors that redundantly contribute to effector-triggered immunity. Plant J. *78*, 978–989.

Markow, A.V. (2005). On the origin of the eukaryotic cell. Paleontol. J. *39*, 109–116.

Martín-Trillo, M., and Cubas, P. (2010). TCP genes: a family snapshot ten years later. Trends Plant Sci. *15*, 31–39.

Micali, C., Göllner, K., Humphry, M., Consonni, C., and Panstruga, R. (2008). The powdery mildew disease of Arabidopsis: A paradigm for the interaction between plants and biotrophic fungi. Arabidopsis Book *6*, e0115.

Mukhtar, M.S., Carvunis, A.-R., Dreze, M., Epple, P., Steinbrenner, J., Moore, J., Tasan, M., Galli, M., Hao, T., Nishimura, M.T., et al.; European Union Effectoromics Consortium (2011). Independently evolved virulence effectors converge onto hubs in a plant immune system network. Science *333*, 596–601.

Nakagawa, T., Kurose, T., Hino, T., Tanaka, K., Kawamukai, M., Niwa, Y., Toyooka, K., Matsuoka, K., Jinbo, T., and Kimura, T. (2007). Development of series of gateway binary vectors, pGWBs, for realizing efficient construction of fusion genes for plant transformation. J. Biosci. Bioeng. *104*, 34–41.

Pais, M., Win, J., Yoshida, K., Etherington, G.J., Cano, L.M., Raffaele, S., Banfield, M.J., Jones, A., Kamoun, S., and Go Saunders, D. (2013). From pathogen genomes to host plant processes: the power of plant parasitic oomycetes. Genome Biol. *14*, 211.

Pardey, P.G., Beddow, J.M., Kriticos, D.J., Hurley, T.M., Park, R.F., Duveiller, E., Sutherst, R.W., Burdon, J.J., and Hodson, D. (2013). Agriculture. Right-sizing stem-rust research. Science *340*, 147–148.

Pedersen, C., Ver Loren van Themaat, E., McGuffin, L.J., Abbott, J.C., Burgis, T.A., Barton, G., Bindschedler, L.V., Lu, X., Maekawa, T., Wessling, R., et al. (2012). Structure and evolution of barley powdery mildew effector candidates. BMC Genomics *13*, 694.

Pieterse, C.M., Van der Does, D., Zamioudis, C., Leon-Reyes, A., and Van Wees, S.C. (2012). Hormonal modulation of plant immunity. Annu. Rev. Cell Dev. Biol. *28*, 489–521.

Raffaele, S., and Kamoun, S. (2012). Genome evolution in filamentous plant pathogens: why bigger can be better. Nat. Rev. Microbiol. *10*, 417–430.

Robert-Seilaniantz, A., Grant, M., and Jones, J.D. (2011). Hormone crosstalk in plant disease and defense: more than just jasmonate-salicylate antagonism. Annu. Rev. Phytopathol. *49*, 317–343.

Spanu, P.D., Abbott, J.C., Amselem, J., Burgis, T.A., Soanes, D.M., Stüber, K., Ver Loren van Themaat, E., Brown, J.K.M., et al. (2010). Genome expansion and gene loss in powdery mildew fungi reveal functional tradeoffs in parasitism. Science *330*, 1543–1546.

Stergiopoulos, I., Kourmpetis, Y.A., Slot, J.C., Bakker, F.T., De Wit, P.J., and Rokas, A. (2012). In silico characterization and molecular evolutionary analysis of a novel superfamily of fungal effector proteins. Mol. Biol. Evol. *29*, 3371–3384.

Sugio, A., Kingdom, H.N., MacLean, A.M., Grieve, V.M., and Hogenhout, S.A. (2011). Phytoplasma protein effector SAP11 enhances insect vector reproduction by manipulating plant development and defense hormone biosynthesis. Proc. Natl. Acad. Sci. USA *108*, E1254–E1263.

Tajima, F. (1989). Statistical method for testing the neutral mutation hypothesis by DNA polymorphism. Genetics *123*, 585–595.

Tamura, K., Peterson, D., Peterson, N., Stecher, G., Nei, M., and Kumar, S. (2011). MEGA5: molecular evolutionary genetics analysis using maximum likelihood, evolutionary distance, and maximum parsimony methods. Mol. Biol. Evol. *28*, 2731–2739.

van der Biezen, E.A., Freddie, C.T., Kahn, K., Parker, J.E., and Jones, J.D. (2002). *Arabidopsis RPP4* is a member of the *RPP5* multigene family of TIR-NB-LRR genes and confers downy mildew resistance through multiple signalling components. Plant J. *29*, 439–451.

Van der Hoorn, R.A., De Wit, P.J., and Joosten, M.H. (2002). Balancing selection favors guarding resistance proteins. Trends Plant Sci. *7*, 67–71.

Watterson, G.A. (1975). On the number of segregating sites in genetical models without recombination. Theor. Popul. Biol. *7*, 256–276.

Weßling, R., Schmidt, S.M., Micali, C.O., Knaust, F., Reinhardt, R., Neumann, U., Ver Loren van Themaat, E., and Panstruga, R. (2012). Transcriptome analysis of enriched *Golovinomyces orontii* haustoria by deep 454 pyrosequencing. Fungal Genet. Biol. *49*, 470–482.

Wicker, T., Oberhaensli, S., Parlange, F., Buchmann, J.P., Shatalina, M., Roffler, S., Ben-David, R., Doležel, J., Šimková, H., Schulze-Lefert, P., et al. (2013). The wheat powdery mildew genome shows the unique evolution of an obligate biotroph. Nat. Genet. *45*, 1092–1096.

Win, J., Chaparro-Garcia, A., Belhaj, K., Saunders, D.G., Yoshida, K., Dong, S., Schornack, S., Zipfel, C., Robatzek, S., Hogenhout, S.A., and Kamoun, S. (2012). Effector biology of plant-associated organisms: concepts and perspectives. Cold Spring Harb. Symp. Quant. Biol. *77*, 235–247.